



Two-Photon Dye Cocktail for Dual-Color 3D Imaging of Pancreatic Beta and Alpha Cells in Live Islets

Bikram Keshari Agrawalla,[†] Hyo Won Lee,[§] Wut-Hmone Phue,[†] Anandhkumar Raju,[‡] Jong-Jin Kim,[†] Hwan Myung Kim,[§] Nam-Young Kang,^{*,‡} and Young-Tae Chang^{*,†,‡} 

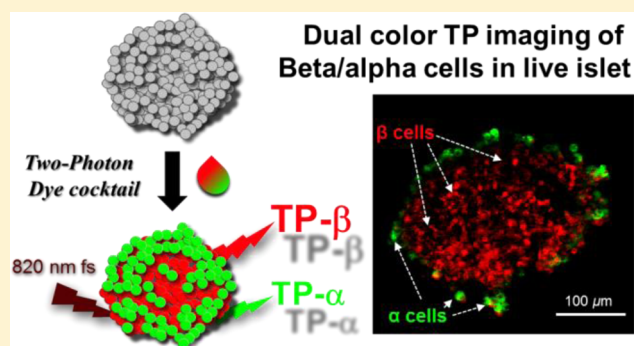
[†]Department of Chemistry and Medicinal Chemistry Program, National University of Singapore, 3 Science Drive 3, 117543 Singapore

[‡]Laboratory of Bioimaging Probe Development, Singapore Bioimaging Consortium, Agency for Science, Technology and Research, 11 Biopolis Way, # 02-02 Helios, 138667 Singapore

[§]Department of Energy Systems Research, Ajou University, Suwon 443749, Korea

 Supporting Information

ABSTRACT: Insulin-secreting beta cells together with glucagon-producing alpha cells play an essential role in maintaining the optimal blood glucose level in the body, so the development of selective probes for imaging of these cell types in live islets is highly desired. Herein we report the development of a 2-glucosamine-based two-photon fluorescent probe, **TP-β**, that is suitable for imaging of beta cells in live pancreatic islets from mice. Flow cytometry studies confirmed that **TP-β** is suitable for isolation of primary beta cells. Moreover, two-photon imaging of **TP-β**-stained pancreatic islets showed brightly stained beta cells in live islets. Insulin enzyme-linked immunosorbent assays revealed that **TP-β** has no effect on glucose-stimulated insulin secretion from the stained islet. Finally, to develop a more convenient islet imaging application, we combined our recently published alpha-cell-selective probe **TP-α** with **TP-β** to make a “TP islet cocktail”. This unique dye cocktail enabled single excitation (820 nm) and simultaneous dual-color imaging of alpha cells (green) and beta cells (red) in live pancreatic islets. This robust TP islet cocktail may serve as a valuable tool for basic diabetic studies.



INTRODUCTION

Pancreatic beta cells are responsible for the production, storage, and release of insulin and thereby regulation of the blood glucose level.¹ Diabetes mellitus, the most common metabolic disorder in humans, is caused by impairment of glucose homeostasis either by autoimmune destruction of insulin-secreting beta cells (type 1)² or peripheral resistance to insulin (type 2).³ Remarkably, our basic understanding of type 1 and type 2 diabetes in humans comes from studies in different rodent models.^{4–6} Most of the antidiabetic drugs, including the popular blood-glucose-lowering oral drug metformin, were developed from studies in a rodent model.^{7,8} For diabetic research, islets from mouse have become a preferred alternative to human tissue, not only because of the ease of availability of mouse islets but also because of their physiological similarities with the latter.^{4–6} The insulin-producing beta cells are situated in islets of Langerhans along with other endocrine cell types, i.e., glucagon-producing alpha cells and somatostatin-producing delta cells.⁹ Islets constitute only about 1–2% of the pancreatic mass and are distributed throughout the whole pancreas.¹⁰ The smaller size (average diameter 100–200 μm) and inaccessible localization of islets have made their *in vivo* study in humans a more challenging task. As a result, the majority of diabetic

studies are performed *in vitro* using live isolated islets or in transplanted conditions.^{11,12} Herein we report the development of a two-photon (TP) fluorescent probe for imaging of beta cells in live intact islets of mice.

Islet imaging has immensely improved our understanding of pancreatic physiology. Two-photon microscopy is becoming a widespread choice for live-tissue imaging because of the deeper tissue penetration of near-infrared excitation lasers.¹³ The development of specific TP fluorescent probes for pancreatic islet cell types could enable researchers to visualize the distribution of alpha, beta, and delta cells in live islets. After our recent discovery of an alpha-cell-selective TP probe, **TP-α** (green emission),¹⁴ we aimed to develop a TP probe for beta cell imaging. The final goal is to achieve dual-color TP imaging of pancreatic beta and alpha cells in live islets. The development of a beta-cell-selective TP probe could be of much value for future diabetic studies.

Inspired by the selective beta-cell-killing capability of the diabetogenic agent streptozotocin (STZ),¹⁵ we designed TP fluorescent probes containing the 2-glucosamine (2-amino-2-

Received: November 24, 2016

Published: February 6, 2017

deoxy-D-glucose) moiety, which is mainly responsible for the beta cell targeting of STZ.¹⁶ Glucose transporter type 2 (Glut2) is the major cell-surface glucose transporter of beta cells in mice,^{17–19} and it has higher affinity for 2-glucosamine over D-glucose.²⁰ Previous reports on the development of probes targeting Glut have emphasized that the linker type and optimum size are crucial for an ideal Glut probe.^{21–24}

The commercially available 2-glucosamine-based fluorescent probe 2-[N-(7-nitrobenz-2-oxa-1,3-diazol-4-yl)amino]-2-deoxy-D-glucose (2-NBDG) has been used for various Glut-related studies.^{25,26} However, in 2-NBDG the fluorophore is directly attached to 2-glucosamine and does not show good competition in cellular uptake with D-glucose.²¹ The high treatment concentration, low sensitivity, and fast photobleaching have made 2-NBDG a less ideal Glut probe.²³ To our knowledge, hitherto no TP fluorescent probe has been demonstrated for beta cell imaging in live intact islets.

We hypothesized that the Glut2-directing 2-glucosamine can be efficiently utilized as a beta cell labeling motif. To evaluate this hypothesis, we synthesized 2-glucosamine (G)-conjugated TP probes. Among the five different linkers, we discovered that the probe containing a six-carbon chain (C6) exhibited higher uptake into mice primary beta cells in comparison with other probes. Next, while evaluating different fluorophores with C6-G, we found that a rhodamine-containing probe (RH-C6-G, denoted as TP- β) is better suited for imaging of beta cells in intact islets. Finally, we combined TP- β with TP- α for dual-color TP imaging of beta and alpha cells in live intact islets.

RESULTS

Synthesis of 2-Glucosamine-Based TP Probes. To have an unbiased study, we made five probes with different linker sizes ranging from zero carbons to 11 carbons (PEG4) between the fluorophore and 2-glucosamine (Figure 1). We chose the

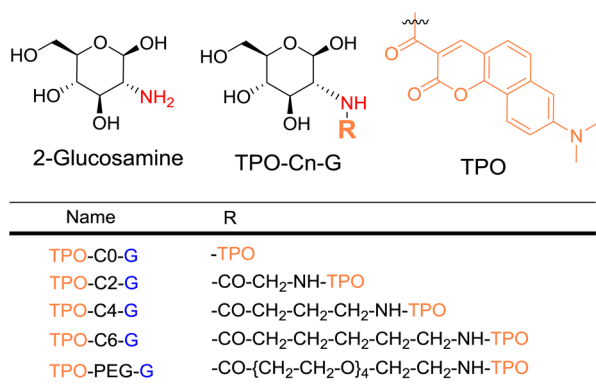


Figure 1. Structures of 2-glucosamine, TPO-C_n-G, and the TPO scaffold.

TP fluorophore 8-(dimethylamino)-2-oxo-2H-benzo[h]-chromene-3-carboxylic acid (DACCA) (TP cross-section = 84 GM at 820 nm, $\Phi = 0.29$) for our synthesis (Figure 1).²⁷ Because of its orange emission (520–600 nm) and TP property, we named this probe “two-photon orange” (TPO) (Figure S2A and S2B). Detailed synthetic procedures for TPO-C0-G, TPO-C2-G, TPO-C4-G, TPO-C6-G, and TPO-PEG-G (Figure S1, Scheme S1 and S2) and their full characterization by ¹H and ¹³C NMR spectroscopy and high-resolution mass spectrometry (HRMS) are available in the Supporting Information.

Cellular Uptake of TPO-C_n-G Probes. A literature review showed that the commercially available insulin-producing beta cell lines Ins1e,²⁸ MIN6,²⁸ and β TC6 have Glut1 (not Glut2) as their major glucose transporter,^{29,30} whereas mice pancreatic beta cells have Glut2 as their major glucose transporter.²⁸ Therefore, primary cells isolated from mice were selected for this study.

Glut2-expressing beta cells constitute the major population of mice pancreatic islets (~70–80%), and the rest are alpha (15–20%) and delta cells (5–10%).³¹ We used whole islet cells for the cell uptake experiment, as the small population of non-Glut2-expressing cells (~20–30% alpha and delta cells together) can act as an internal negative control. Islets from mice pancreas were isolated by the collagenase P method as described elsewhere.³² The isolated islets were dissociated to single cells for the cell uptake study.

Flow cytometry was used for quantitative measurement of TPO-C_n-G uptake into the dissociated islet cells. The islet cells were incubated with 5 μ M TPO-C_n-G compounds for 2 h at 37 °C (in Dulbecco’s modified Eagle’s medium (DMEM) containing 10 mM D-glucose under 5% CO₂) before the intensity measurement. As shown in Figure 2A, the different TPO-C_n-G compounds exhibited differential uptakes into the islet cells. We observed that three glucosamine analogues, TPO-C2-G, TPO-C4-G, and TPO-C6-G, gave similar population separations of $\sim 74 \pm 3\%$ bright cells and $\sim 23 \pm 2\%$ dim cells (Figure 2A, panels c–e, and Figure 2B). As anticipated, this population of $\sim 75\%$ bright cells is pertinent

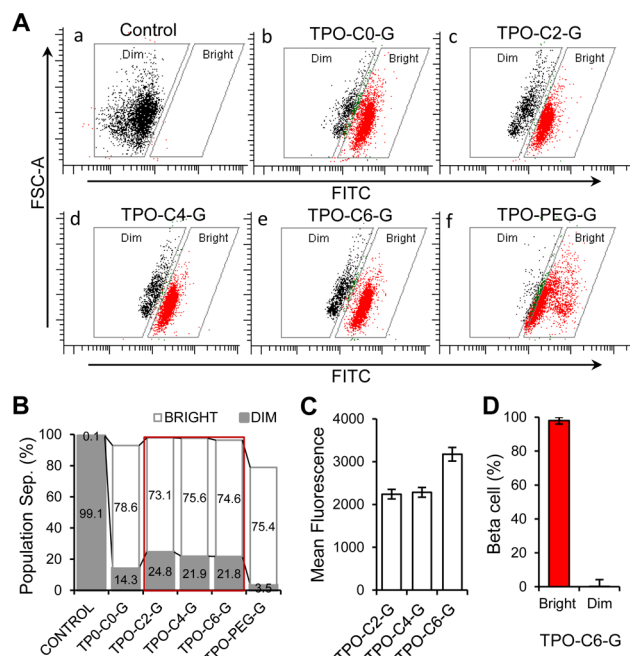


Figure 2. Islet cell staining with TPO-C_n-G probes. (A) Flow cytometry dot plots showing the population distributions for dissociated islet cells stained with 5 μ M TPO-C_n-G compounds for 2 h at 37 °C in DMEM containing 10 mM D-glucose. Control cells were incubated without dye. Dim regions are coded in black and bright regions in red. (B) Bar diagram for the dim and bright cell populations in percentage corresponding to each plot in (A). (C) Mean fluorescence intensities of cells in the bright-gated regions of panels c–e in (A). (D) Insulin-positive cell populations for TPO-C6-G bright and dim cells (the flow cytometry data are shown in Figure S4). Each dot plot/bar diagram represents 10 000 islet cell counts.

to the beta cell population in the pancreatic islet (70–85%).³¹ However, for TPO-C0-G and TPO-PEG-G, the dim and bright cells were not well-separated (Figure 2A, panels b and f, and Figure 2B). To further identify the best compound among TPO-C2-G, TPO-C4-G, and TPO-C6-G, we measured the fluorescence intensities of the cells in the dye bright-gated region. We found the TPO-C6-G bright cells to have ~30% higher fluorescence compared with TPO-C2-G and TPO-C4-G (Figure 2C), reflecting the higher dye uptake, as these probes have almost identical quantum yields (Table S2). This increased dye uptake resulted in comparatively better cell separation between the TPO-C6-G dim and bright populations compared with the other tested probes (Figure 2A, panel e). These data suggested that tuning the size of the linker between the targeting motif (2-glucosamine) and the fluorophore could result in a higher-uptake probe. Finally, because of its better population separation and higher uptake (~30% over the C2 and C4 analogues), we chose the C6-linker-containing compound (TPO-C6-G) for our further studies. Insulin antibody staining revealed that TPO-C6-G bright cells are insulin-positive beta cells (Figures 2D and S4).

Islet Staining with TPO-C6-G. Next, we targeted the imaging of beta cells in intact live islets. TP imaging of intact islets stained with TPO-C6-G showed that the dye-stained cells were located at the edge of the islet and had poor access to the center (Figure 3A, panels a and d, and Figure 3B). Takahashi et al.³³ observed such a pattern for islet imaging with hydrophobic dyes. Thus, we believed that the hydrophobic benzo[*h*]-chromene core of TPO-C6-G (cLogP = 1.41) could be

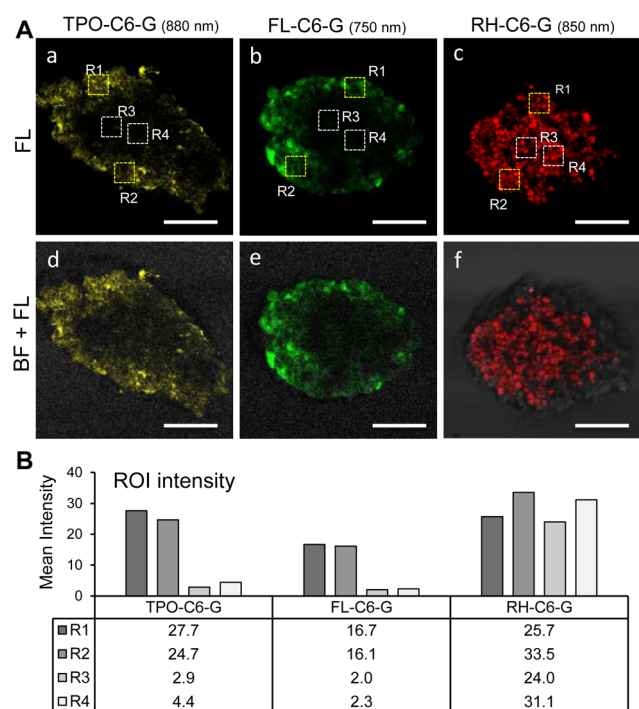


Figure 3. (A) TP fluorescence (FL) images of islets stained with (a) TPO-C6-G, (b) FL-C6-G, and (c) RH-C6-G incubated with 10 μ M dye at 37 $^{\circ}$ C for 2 h in DMEM containing 10 mM D-glucose. (d–f) Merged bright-field (BF) + FL images of the islets. Scale bars = 100 μ m. (B) Mean intensities from regions of interest (ROIs) for the islets in panels a–c in (A): R1 and R2 (outer regions, yellow border) and R3 and R4 (central regions, white border). Intensities were measured using FIJI ImageJ.

accountable for this behavior. Nevertheless, the same report demonstrated that hydrophilic dyes have better entry to the center of the islet.³³ To evaluate whether this behavior was due to the hydrophobic benzo[*h*]chromene core, we planned to synthesize two new C6-G probes containing hydrophilic and hydrophobic fluorescent cores. If the hydrophobic probe showed a similar staining pattern to TPO-C6-G whereas the hydrophilic probe had better access to the center of the islets, this would confirm that the superficial staining of TPO-C6-G was due to hydrophobicity.

Synthesis of New C6-G probes. We synthesized two new C6-G probes containing hydrophilic (rhodamine: RH-C6-G, cLogP = 1.03) and hydrophobic (fluorescein: FL-C6-G, cLogP = 1.75) fluorescent cores (Figure 4A).³⁴ Detailed synthetic

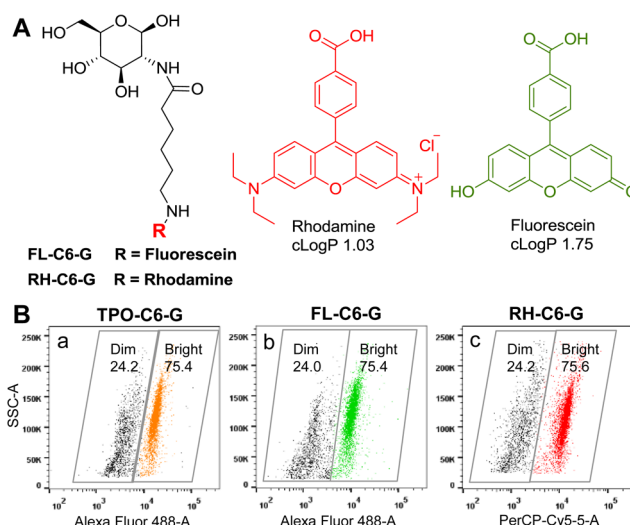


Figure 4. (A) Structures of FL-C6-G and RH-C6-G. (B) Flow cytometry dot plots for dissociated islet cells stained with 5 μ M (a) TPO-C6-G, (b) FL-C6-G, and (c) RH-C6-G for 2 h at 37 $^{\circ}$ C in DMEM containing 10 mM D-glucose. Each dot plot represents 10 000 islet cell counts.

procedures (Schemes S3 and S4) and photophysical data and chemical characterization by 1 H and 13 C NMR spectroscopy and HRMS are available in the Supporting Information. FL-C6-G and RH-C6-G have green and red emission, respectively (Figure S2C). The TP action cross section of RH-C6-G is 120 GM at 850 nm, and that of FL-C6-G is 20 GM at 770 nm (Figure S2D). First we analyzed the cell uptake efficiencies of these C6-G probes with flow cytometry using dissociated islet cells. The three C6-G probes (TPO-C6-G, FL-C6-G, and RH-C6-G) (Figure S3) exhibited similar performance and showed 75 \pm 2% bright cell population separation (Figure 4B). These results suggest that the efficiency is similar for staining of dissociated islet cells with hydrophobic TPO-C6-G (cLogP = 1.4) and FL-C6-G (cLogP = 1.7) and hydrophilic RH-C6-G (cLogP = 1). However, the ideal probe should be able to stain beta cells present in the intact live islets.

Next, we determined the adeptness of these probes for accessibility into intact islets. Live islets stained with FL-C6-G showed performance similar to that of cells stained with TPO-C6-G, with poor penetration to the core of the islet (Figure 3A, panels b and e, and Figure 3B). In contrast, RH-C6-G exhibited good access to the center of the islet (Figure 3A, panels c and f, and Figure 3B). The mean intensity profiles of TPO-C6-G- and FL-C6-G-stained islets show weaker dye signals from the

central regions (R3 and R4; Figure 3B) in comparison with the cells in the outer layer of the islets (R1 and R2). In contrast, the intensity profile of RH-C6-G-stained islets shows consistent fluorescence signals from cells throughout the islet (Figure 3A,B). This result supports our hypothesis that C6-G probes containing hydrophobic fluorophores (TPO-C6-G and FL-C6-G) exhibit poor penetration into the islets, whereas the hydrophilic probe (RH-C6-G) has better access to the center of the islet. These findings are in good agreement with the literature report.³³ The desired population separation of ~75% bright cells in flow cytometry and good penetration to the center of the islet makes RH-C6-G the most suitable candidate for beta cell imaging in live intact islets, so we renamed RH-C6-G as TP- β .

TP- β Stains Pancreatic Beta Cells in Intact Islets. Flow cytometry analysis of TP- β (RH-C6-G)-stained dissociated islet cells showed $75 \pm 3\%$ bright cells (Figure 4B, panel c), whereas the intact islet staining showed $74 \pm 2\%$ TP- β bright cells (Figure 5A). These results indicate that TP- β can selectively

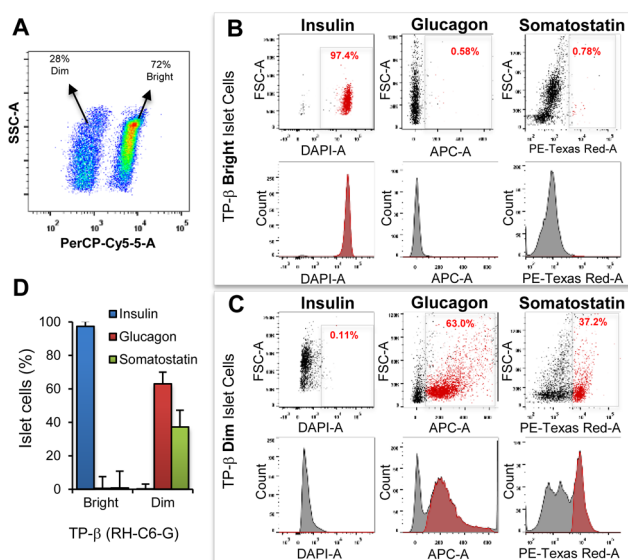


Figure 5. TP- β stains beta cells in intact islets. (A) Intact islet stained with $10 \mu\text{M}$ TP- β for 2 h at 37°C in DMEM containing 10 mM D-glucose followed by dissociation, fluorescence-activated cell sorting, and immunostaining. (B) Insulin, glucagon, and somatostatin antibody staining of TP- β bright islet cells. (C) Immunostaining of TP- β dim islet cells. The gated region (red) represents the antibody-positive population. (D) Bar diagram for antibody-positive islet cells of TP- β bright and TP- β dim cells. More than 100 000 islet cells were sorted. The spectra in (B) and (C) reflect cell counts of 10 000 each.

stain similar populations by staining of either intact or dissociated islets. For characterization, we stained intact islets with TP- β and sorted out the bright and dim cells for antibody characterization (Figure 5A). The majority of TP- β bright cells were insulin-antibody-positive with an accuracy of 97%, whereas negligible cells were either glucagon- or somatostatin-antibody-positive (~1.5% combined) (Figure 5B). Similarly, the entire population (99%) of TP- β dim cells were insulin-antibody-negative and consisted of glucagon-containing alpha cells and somatostatin-containing delta cells (Figure 5C). The bar diagram in Figure 5D clearly shows that TP- β bright cells are beta cells whereas the dim cells are alpha and delta cells. The antibody characterization confirms that TP- β staining of

intact islets can selectively stain the beta cells and does not stain the other endocrine cell types.

Dual-Color TP Imaging of Alpha and Beta Cells in Live Islets. Our final goal was to perform dual-color TP imaging of alpha and beta cells in live intact islets. Our recently published probe TP- α selectively stains glucagon-containing alpha cells in live intact islets.¹⁴ We planned to assess the performance of TP- α and TP- β together (Figure 6A). The TP measurement shows that both TP- α and TP- β have action cross-sections of ~60 GM at 820 nm and are suitable for dual excitation at this wavelength (Figure 6B). In contrast, Figure 6C shows exclusive emission windows for TP- α (430–530 nm) and TP- β (550–650 nm). These photophysical characterizations suggest that the TP- β and TP- α dye combination is suitable for dual-color TP imaging. As expected, the flow cytometry study of TP- β + TP- α stained intact islets showed three distinct populations: 72% TP- β -positive beta cells, 15% TP- α -positive alpha cells, and the remaining dual-negative population of 12% representing the delta cells (Figure 6F). Because of its usefulness, we named this dye combination as the “TP islet cocktail”, which can be efficiently used for staining mice pancreatic beta cells in red color and alpha cells in green color.

Fresh islets stained with TP islet cocktail ($0.5 \mu\text{M}$ TP- α + $10 \mu\text{M}$ TP- β) show red-emitting beta cells at the core of the islet, whereas green-emitting alpha cells appear at the surface of the islet (Figure 6D, panel c). The TP images in the TP- β channel show individual beta cells at the core of the islet with bright TP- β signal (Figure 6D, panels b and c), whereas TP- α -stained surface-localized alpha cells are TP- β dim/negative (arrowheads in Figure 6D, panels a–c). The Z-stack projection of the whole islet clearly demonstrates the exclusive green and red signals from specific cells of the intact islet. Similarly, the 3D surface projection shows distinguishable alpha and beta cells labeled with TP- α and TP- β , respectively (Figure 6E).

DISCUSSION

Technological advancement in TP microscopy has created a high demand for the development of novel TP bioimaging probes.^{36,37} Islets isolated from transgenic mice models with the fluorescent protein expressed in beta cells are frequently used for beta cell/islet imaging studies.^{37,38} However, it is well-known that the development of transgenic models and their maintenance are both tedious and expensive. Hence, small-molecule fluorescent probes that can selectively stain beta cells in isolated islets can offer a convenient alternative to fluorescent protein expression in beta cells for cell imaging studies. Herein we report the development of a beta-cell-targeting TP fluorescent probe that can selectively stain insulin-producing beta cells in isolated islets from mice. The selectivity of streptozotocin toward mice beta cells inspired us to use its 2-glucosamine targeting motif to design a beta-cell-imaging probe.^{15,16}

We optimized both the linker size and the fluorophore to develop a suitable islet imaging probe. Among the five different linkers, the C6-containing probe (TPO-C6-G) demonstrated desired cell separation and higher uptake into the mice primary beta cells (Figure 2). However, imaging of islets stained with TPO-C6-G revealed that the dye has poor access to the center of the islet (Figure 3). Islets are spheres of tightly packed endocrine cells, and hydrophobic dyes have been reported to have poor access to its core.³³ Following this observation, we next developed two more C6-G probes with hydrophilic

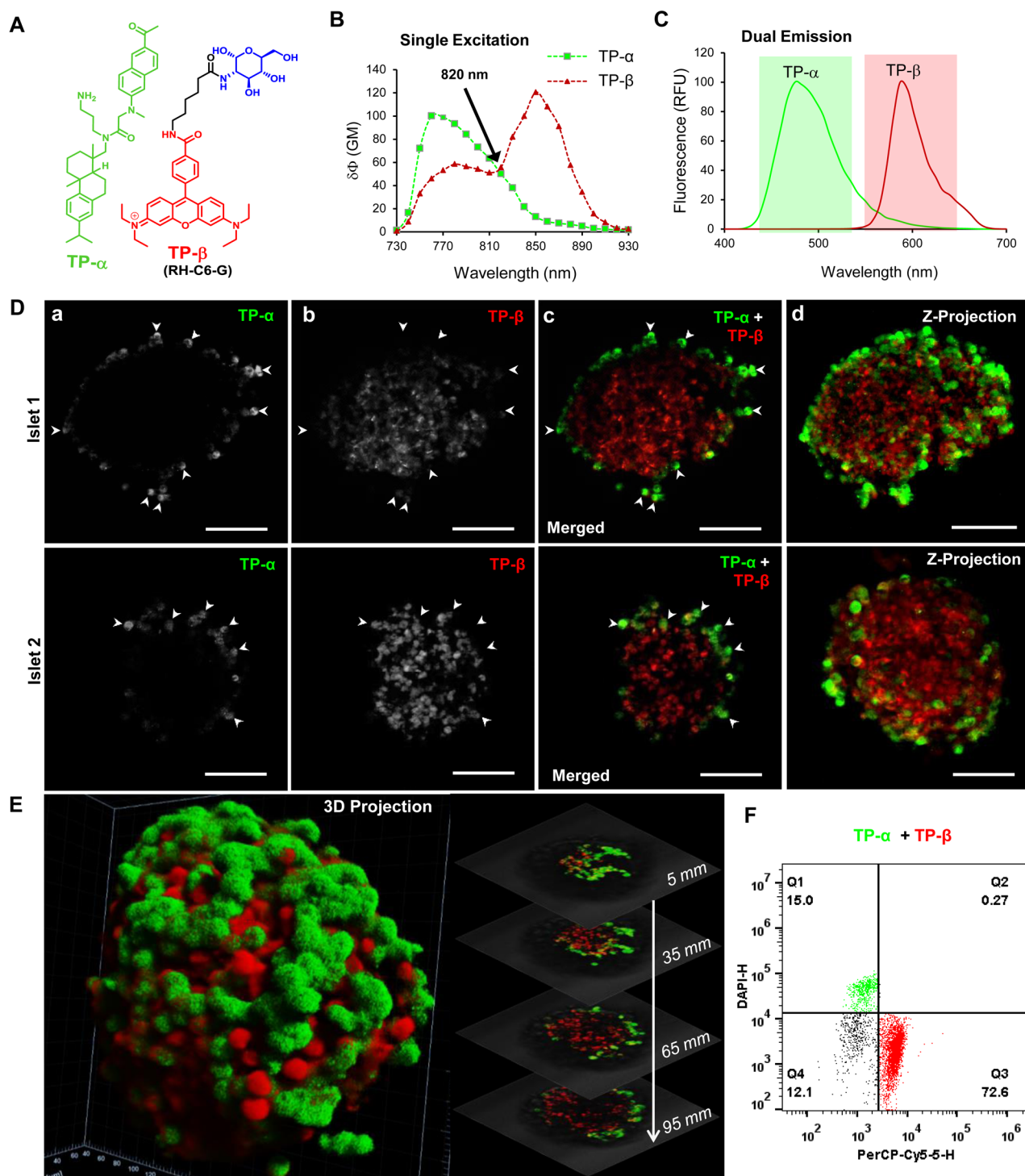


Figure 6. Dual-color two-photon imaging of pancreatic islets stained with the “TP islet cocktail”. (A) Structures of TP- β (RH-C6-G) and TP- α . (B) TP action spectra of TP- β and TP- α . (C) Fluorescence emission spectra of TP- β (550–650 nm, red) and TP- α (430–530 nm, green) showing the exclusive detection windows. (D) TP images of live pancreatic islets stained with the TP islet cocktail (10 μ M TP- β + 0.5 μ M TP- α): (a) TP- α signal (430–530 nm); (b) TP- β signal (550–650 nm); (c) merged image of the two channels. Arrowheads indicate that the TP- α bright alpha cells are TP- β negative (dim). (d) Z projection of the whole islet showing the distribution of alpha cells on the surface of the islet. Scale bar = 150 μ m. (E) 3D surface projection of the TP Z-stack images for a live islet stained with TP islet cocktail (step size = 0.17 μ m) using IMARIS image processing software. Representative sectional overlaid TP images of the live islet over the depth range of 5–95 μ m are also shown. Excitation was done at 820 nm using a femtosecond laser; TP- α and TP- β emissions were monitored at 430–530 and 550–650 nm, respectively. Images are representative of $n = 50$ islets. (F) TP islet cocktail-stained islet cells showing population separation for three different cell types. Live pancreatic islets were stained with TP islet cocktail (10 μ M TP- β + 0.5 μ M TP- α) and incubated for 2 h at 37 $^{\circ}$ C in DMEM containing 10 mM D-glucose before analysis. The results reflect cell counts of 10 000.³⁵

(rhodamine: RH-C6-G, cLogP = 1.03) and hydrophobic (fluorescein: FL-C6-G, cLogP = 1.75) probes.

TP imaging of intact islets with these probes demonstrated that the probe containing C6-G with the hydrophilic fluorophore (RH-C6-G, TP- β) had better access to the islet core and can stain beta cells brightly even at the center of the islet (Figure 3A, panels c and f, and Figure 3B). This behavior of TP- β can be assigned to its greater water solubility, which enables access of the dye to the center of the islet through the capillary blood vessels present in the freshly isolated islets. However, the hydrophobic dyes (TPO-C6-G and FL-C6-G) have greater affinity for the plasma membrane and may get entrapped in the lipid membranes of cells/capillary blood vessels localized on the surface of the islet.

Equipped with these findings, we sought to explore the possibility of dual-color imaging of beta and alpha cells in live intact islets. For this purpose, we combined TP- β (RH-C6-G) with TP- α (our recently published alpha-cell-selective TP fluorescent probe)¹⁴ and denoted the mixture as the “TP islet cocktail” (Figure 6A). The photophysical study revealed that the TP islet cocktail is suitable for single TP excitation (820 nm) and dual emission (exclusive channels) (Figure 6B,C). To our delight, islets stained with the TP islet cocktail showed brightly stained alpha and beta cells in green and red emission windows, respectively (Figure 6D). TP imaging enabled dual-color 3D imaging of live islets, which showed brightly stained alpha and beta cells in two different colors (Figure 6E). This is the first demonstration of dual-color two-photon imaging of alpha and beta cells in live intact islets with islet-cell-selective small-molecule two-photon fluorescent probes.

Subsequently, to confirm that the TP- β uptake into beta cells is Glut-mediated, we performed a competition assay with increasing concentrations of D-glucose with islet cells. To our delight, the uptake of TP- β concentration-dependently decreased with increasing concentration of D-glucose (Figure S5), providing evidence for the glucose-transporter-mediated uptake of TP- β .

After validating the Glut-mediated uptake of TP- β to the beta cells, we compared it with the commercially available fluorescent glucosamine-based probe 2-NBDG. When we compared the uptake of 2-NBDG (10 μ M) with that of TP- β (10 μ M) to the islet cells, we found TP- β to exhibit considerably higher uptake than 2-NBDG (Figure S6). Furthermore, we doubled the concentration of 2-NBDG (20 μ M), but still the fluorescence intensity reached only 30% of that of TP- β -treated cells (Figure S6). This experiment demonstrates significantly higher uptake of TP- β by beta cells in comparison with 2-NBDG.

One of the prime uses of isolated islets is to study insulin secretion under various test conditions.³⁹ Hence, we evaluated the secretion of insulin from TP- β -stained islets. The insulin enzyme-linked immunosorbent assay (ELISA) revealed that the TP- β staining does not affect the insulin secretion of the islets (Figure 7). Moreover, a cell viability study of TP- β -stained islet cells from mice showed minimal cytotoxicity in the working concentration range of the dye (Figure S7). These findings suggest that TP- β can also be combined with insulin secretion assays of islets with minimal toxicity to the endocrine cells.

CONCLUSION

We have developed a 2-glucosamine-based fluorescent probe, TP- β , that is suitable for beta cell imaging in live intact islets from mice. During the development of TP- β , various linkers

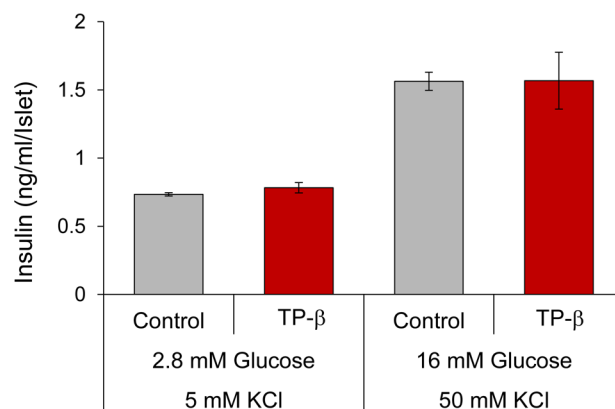


Figure 7. TP- β staining does not affect insulin secretion. The control and 10 μ M TP- β -stained islets show similar insulin secretion under both nonstimulatory and stimulatory conditions.

and fluorophores were evaluated to find the most suitable islet imaging probe. TP- β not only can efficiently stain beta cells in live islets but also is suitable for isolation of primary beta cells. TP- β and TP- α together enable dual-color imaging of beta and alpha cells in live islets using single TP excitation. An insulin ELISA revealed that TP- β staining does not interfere with insulin secretion from the islet. Moreover, a cell viability study highlighted that TP- β has minimal toxicity. While mice models remain as the most studied platform for diabetic research, this probe may prove to be a very robust and useful tool in diabetes studies.

EXPERIMENTAL DETAILS

Quantum Yield Measurements. Quantum yields were calculated by measuring the integrated area of emission spectra for synthesized compounds (including TP- β) in comparison to the same measurement for rhodamine B ($\Phi = 0.58$) in dimethyl sulfoxide as a reference compound.⁴⁰ Quantum yields were calculated using eq 1:

$$\Phi_{\text{sample}} = \Phi_{\text{ref}} \frac{F_{\text{sample}} \eta_{\text{sample}} \text{Abs}_{\text{ref}}}{F_{\text{ref}} \eta_{\text{ref}} \text{Abs}_{\text{sample}}} \quad (1)$$

where Φ is the quantum yield, F is the area of fluorescence emission, η is the refractive index of the solvent, and Abs is the absorbance at the excitation wavelength.⁴¹

Two-Photon Absorption Cross Section Measurements. The TP emission spectra of synthesized compounds were determined over a broad spectral region by the TP-induced fluorescence (TPF) method with rhodamine B in methanol as a reference.³⁵ A PTI Quanta Master spectrofluorimeter and a Coherent Mira 900F femtosecond Ti:sapphire laser (220 fs pulse width, 76 MHz repetition rate, tuning range 700–1000 nm) were used. TP fluorescence measurements were performed in 10 mm fluorometric quartz cuvettes with 10 μ M TP- β in methanol and 10 μ M rhodamine B as a reference in the same solvent. The experimental fluorescence excitation and detection conditions were chosen to ensure negligible reabsorption processes, which can affect TPA measurements. The TP absorption cross sections of the probes were calculated at each wavelength according to eq 2:

$$\delta_{\text{sample}} = \delta_{\text{ref}} \frac{\Phi_{\text{ref}} I_{\text{sample}} C_{\text{ref}} \eta_{\text{sample}}^2 P_{\text{ref}}^2}{\Phi_{\text{sample}} I_{\text{ref}} C_{\text{sample}} \eta_{\text{ref}}^2 P_{\text{sample}}^2} \quad (2)$$

where δ is the cross section, I is the integrated fluorescence intensity, C is the concentration, η is the refractive index, Φ is the quantum yield, and P is the incident power. The uncertainty in the measured cross sections was about $\pm 10\%$.

Islet Isolation and Imaging. Primary pancreatic islets were isolated from 10–16 week old C57BL/6 (WT) male mice. The animal

handling and tissue harvesting were done in accordance with the Institutional Animal Care and Use Committee of Singapore Bioimaging Consortium (Agency of Science, Technology and Research, Singapore). Pancreatic islets were isolated by collagenase P digestion and islet picking methods as described earlier.³² Briefly, fresh pancreas was cut into small pieces and digested with 1 mg/mL collagenase P (Roche, Indianapolis, IN) solution in Hank's balanced salt solution (HBSS) (Invitrogen) for 10 min at 37 °C in DMEM with 10 mM D-glucose on a shaker, followed by four washes with buffer to remove the digested exocrine tissue. Manual picking of pancreatic islets was carried out using a Zeiss Stemi DV4 stereomicroscope. Islets were maintained in DMEM with 10 mM D-glucose plus 10% fetal bovine serum (FBS) and 1% penicillin–streptomycin (GIBCO, Life Technologies, Carlsbad, CA) before TP imaging. Islets were stained with TP islet cocktail (0.5 μ M TP- α + 10 μ M TP- β) for 2 h at 37 °C in DMEM with 10 mM D-glucose and transferred to fresh medium for TP image acquisition.

Dissociation of Islets. Primary pancreatic islet cells were dissociated by the trypsinization and trituration method.³² Approximately 100–150 islets were dissociated by incubation with 0.25% trypsin-EDTA (1 \times) and phenol red (GIBCO) at 37 °C for 2 min, followed by trituration with repeated pipetting. Finally, the dissociated islet cells were transferred to DMEM containing 10 mM D-glucose plus 10% FBS and 1% penicillin–streptomycin for culture. The cells were stained with 5 μ M TPO-C α -G probes for 2 h at 37 °C and were transferred to fresh medium before flow cytometry studies.

Two-Photon Imaging. All TP imaging was done using a Leica TCS SP5X MP system (Leica Microsystems CMS GmbH, Mannheim, Germany) with an 820 nm pulsed femtosecond laser for dual TP excitation of TP- β and TP- α . Images were taken using 40 \times water objectives. TP excitation of the TP islet cocktail was achieved using a Ti:sapphire laser light set at a wavelength of 820 nm and an output power of 2710 mW. To obtain the probe signal, the internal photomultiplier tube was set at 550–650 nm for TP- β and at 430–530 nm for TP- α . Image analysis and intensity measurements were carried out using Leica Application Suite Advanced Fluorescence (LAS AF). The 3D projection of Z-stack TP images was processed with IMARIS software (Bitplane AG, Zürich, Switzerland), and the intensity is depicted as false color.

Immunostaining. Primary cells and islets were fixed in 4% paraformaldehyde and permeabilized with 0.1% Triton-X 100. Fixed cells were identified by primary antibodies against secretory markers at the respective dilutions. For beta cells, polyclonal guinea pig anti-insulin antibody (DAKO North America, Carpinteria, CA, USA) 1:200 and anti-guinea pig immunoglobulin G (IgG) (H+L) 405 nm were used for secondary antibody staining. For alpha cells, monoclonal mouse antiglucagon antibody (Sigma-Aldrich, St. Louis, MO, USA) 1:2000 and Cy5 goat anti-mouse IgG (Invitrogen, Molecular Probes Inc., USA) 1:200 were used as secondary antibodies. For delta cells, polyclonal rabbit anti-human somatostatin antibody (DAKO North America) and Alexa Fluor 488 goat anti-rabbit IgG (H+L) secondary antibody were used. Cells were analyzed using a BD LSR II analyzer flow cytometer.

Cytotoxicity Assays. Cytotoxicity assays were carried out using the MTS reagent kit (Promega) for 1–48 h with 1–100 μ M TP- β -treated primary islet cells in accordance with the manufacturer's instructions.

Flow Cytometry. Primary islets cells were obtained from 10–16 week old C57BL/6 (WT) male mice as described above. Cells were stained with 5 μ M TP- β for 2 h at 37 °C in DMEM with 10 mM D-glucose and washed with phosphate-buffered saline (PBS) before acquisition on the BD LSR II analyzer. Cells were acquired using the appropriate filters for TP- β (BD PerCP Cy5.5; excitation laser light at 488 nm and emission at 695/40 nm).

Insulin ELISA. Insulin ELISA was performed as discussed elsewhere.³⁹ In each Eppendorf tube were placed 10 islets of similar diameter (100–150 μ m), and each condition was triplicated. Islets were incubated with 10 μ M TP- β in DMEM containing 10 mM D-glucose for 2 h at 37 °C, and unstained islets were used as a control. Islets were washed with PBS before transfer into 100 μ L of KREBS

buffer containing 2.8 mM D-glucose and 5 mM calcium and incubated at 37 °C for 1 h. The tubes were centrifuged at 1000 rpm, and the supernatant was collected for insulin measurement. After PBS washing, islets were stimulated with a fresh 100 μ L of KREBS medium containing 16 mM D-glucose and 50 mM calcium and incubated at 37 °C for 1 h, followed by medium collection for insulin measurement. Insulin concentrations in the collected fractions were measured using the Mercodia Mouse Insulin ELISA. The reading is the concentration of insulin in ng/mL of medium. After calculation of the absolute amount of insulin in the medium volume, this amount was divided by 10 (the number of islets in the tube, which were of similar size). The size (diameter) was measured during islet selection using a camera mounted on a stereomicroscope.

■ ASSOCIATED CONTENT

📄 Supporting Information

The Supporting Information is available free of charge on the ACS Publications website at DOI: 10.1021/jacs.6b12122.

Detailed experimental procedures and chemical characterization (PDF)

■ AUTHOR INFORMATION

Corresponding Authors

*kang_nam_young@sbic.a-star.edu.sg

*chmcyt@nus.edu.sg

ORCID

Young-Tae Chang: 0000-0002-1927-3688

Notes

The authors declare no competing financial interest.

■ ACKNOWLEDGMENTS

The authors thank Ms. Tong Yan of the NUS Centre of Bio-Imaging Science for the Two-Photon Imaging Facility. The authors thank Mr. Daniel Anand Silva and Ms. Najwa Binte Said Nasir Talib of The Biomedical Sciences Institute, Agency for Science, Technology and Research for the Flow-cytometry facility. This study was supported by intramural funding from the Joint Council Office (JCO) Career Development Award (CDA) and the Agency for Science, Technology and Research, Singapore (A*STAR) (15302FG148). H.M.K. acknowledges a grant from the Human Resources Development of the KETEP Grant from the Government of Korea (20154010200820).

■ REFERENCES

- (1) Saudek, F.; Brogren, C. H.; Manohar, S. *Rev. Diabet. Stud.* **2008**, *5*, 6.
- (2) Van Belle, T. L.; Coppieters, K. T.; von Herrath, M. G. *Physiol. Rev.* **2011**, *91*, 79.
- (3) Lin, Y.; Sun, Z. *J. Endocrinol.* **2010**, *204*, 1.
- (4) King, A. J. F. *Br. J. Pharmacol.* **2012**, *166*, 877.
- (5) Atkinson, M. A.; Leiter, E. H. *Nat. Med.* **1999**, *5*, 601.
- (6) Leiter, E. H. *ILAR J.* **1993**, *35*, 4.
- (7) Zavaroni, I.; Aglio, E. D.; Coscelli, C. *Diabetologia* **1981**, *21*, 345.
- (8) Frayn, K. N. *Diabetologia* **1976**, *12*, 53.
- (9) Leibiger, I. B.; Leibiger, B.; Berggren, P. O. *Annu. Rev. Nutr.* **2008**, *28*, 233.
- (10) Speier, S.; Nyqvist, D.; Kohler, M.; Caicedo, A.; Leibiger, I. B.; Berggren, P. O. *Nat. Protoc.* **2008**, *3*, 1278.
- (11) Kahraman, S.; Dirice, E.; Hapil, F. Z.; Ertosun, M. G.; Ozturk, S.; Griffith, T. S.; Sanlioglu, S.; Sanlioglu, A. D. *Diabetes/Metab. Res. Rev.* **2011**, *27*, 575.
- (12) Speier, S.; Nyqvist, D.; Cabrera, O.; Yu, J.; Molano, R. D.; Pileggi, A.; Moede, T.; Kohler, M.; Wilbertz, J.; Leibiger, B.; Ricordi, C.; Leibiger, I. B.; Caicedo, A.; Berggren, P. O. *Nat. Med.* **2008**, *14*, 574.

- (13) Dunn, K. W.; Sutton, T. A. *ILAR J.* **2008**, *49*, 66.
- (14) Agrawalla, B. K.; Chandran, Y.; Phue, W. H.; Lee, S. C.; Jeong, Y. M.; Wan, S. Y.; Kang, N. Y.; Chang, Y. T. *J. Am. Chem. Soc.* **2015**, *137*, 5355.
- (15) Herr, R. R.; Eble, T. E.; Bergy, M. E.; Jahnke, H. K. *Antibiot. Annu.* **1959**, *7*, 236.
- (16) Herr, R. R.; Jahnke, J. K.; Argoudelis, A. D. *J. Am. Chem. Soc.* **1967**, *89*, 4808.
- (17) Hosokawa, M.; Dolci, W.; Thorens, B. *Biochem. Biophys. Res. Commun.* **2001**, *289*, 1114.
- (18) Wang, Z.; Gleichmann, H. *Diabetes* **1998**, *47*, 50.
- (19) Takeda, J.; Kayano, T.; Fukumoto, H.; Bell, G. I. *Diabetes* **1993**, *42*, 773.
- (20) Uldry, M.; Ibberson, M.; Hosokawa, M.; Thorens, B. *FEBS Lett.* **2002**, *524*, 199.
- (21) Tian, Y. S.; Lee, H. Y.; Lim, C. S.; Park, J.; Kim, H. M.; Shin, Y. N.; Kim, E. S.; Jeon, H. J.; Park, S. B.; Cho, B. R. *Angew. Chem., Int. Ed.* **2009**, *48*, 8027.
- (22) Zhang, M.; Zhang, Z.; Blessington, D.; Li, H.; Busch, T. M.; Madrak, V.; Miles, J.; Chance, B.; Glickson, J. D.; Zheng, G. *Bioconjugate Chem.* **2003**, *14*, 709.
- (23) Park, J.; Um, J. I.; Jo, A.; Lee, J.; Jung, D. W.; Williams, D. R.; Park, S. B. *Chem. Commun.* **2014**, *50*, 9251.
- (24) Lee, H. Y.; Lee, J. J.; Park, J.; Park, S. B. *Chem. - Eur. J.* **2011**, *17*, 143.
- (25) Yoshioka, K.; Takahashi, H.; Homma, T.; Saito, M.; Oh, K. B.; Nemoto, Y.; Matsuoka, H. *Biochim. Biophys. Acta, Gen. Subj.* **1996**, *1289*, 5.
- (26) Yamada, K.; Nakata, M.; Horimoto, N.; Saito, M.; Matsuoka, H.; Inagaki, N. *J. Biol. Chem.* **2000**, *275*, 22278.
- (27) Kim, H. M.; Yang, P. R.; Seo, M. S.; Yi, J. S.; Hong, J. H.; Jeon, S. J.; Ko, Y. G.; Lee, K. J.; Cho, B. R. *J. Org. Chem.* **2007**, *72*, 2088.
- (28) Kaminski, M. T.; Lenzen, S.; Baltrusch, S. *Biochim. Biophys. Acta, Mol. Cell Res.* **2012**, *1823*, 1697.
- (29) Tal, M.; Thorens, B.; Surana, M.; Fleischer, N.; Lodish, H. F.; Hanahan, D.; Efrat, S. *Mol. Cell Biol.* **1992**, *12*, 422.
- (30) Arya, A.; Looi, C. Y.; Cheah, S. C.; Mustafa, M. R.; Mohd, M. A. *J. Ethnopharmacol.* **2012**, *144*, 22.
- (31) Steiner, D. J.; Kim, A.; Miller, K.; Hara, M. *Islets* **2010**, *2*, 135.
- (32) Lernmark, A. *Diabetologia* **1974**, *10*, 431.
- (33) Takahashi, N.; Nemoto, T.; Kimura, R.; Tachikawa, A.; Miwa, A.; Okado, H.; Miyashita, Y.; Iino, M.; Kadowaki, T.; Kasai, H. *Diabetes* **2002**, *51* (Suppl. 1), S25.
- (34) Song, B.; Wu, C.; Chang, J. J. *Biomed. Mater. Res., Part B* **2012**, *100B*, 2178.
- (35) Kauert, M.; Stoller, P. C.; Frenz, M.; Ricka, J. *Opt. Express* **2006**, *14*, 8434.
- (36) Helmchen, F.; Denk, W. *Nat. Methods* **2005**, *2*, 932.
- (37) Hara, M.; Wang, X.; Kawamura, T.; Bindokas, V. P.; Dizon, R. F.; Alcoser, S. Y.; Magnuson, M. A.; Bell, G. I. *Am. J. Physiol. Endocrinol. Metab.* **2003**, *284*, E177.
- (38) Leibiger, I. B.; Caicedo, A.; Berggren, P. O. *Acta Physiol.* **2012**, *204*, 178.
- (39) Geng, X.; Li, L.; Bottino, R.; Balamurugan, A. N.; Bertera, S.; Densmore, E.; Su, A.; Chang, Y.; Trucco, M.; Drain, P. *Am. J. Physiol. Endocrinol. Metab.* **2007**, *293*, E293.
- (40) Xu, C.; Zipfel, W.; Shear, J. B.; Williams, R. M.; Webb, W. W. *Proc. Natl. Acad. Sci. U. S. A.* **1996**, *93*, 10763.
- (41) Ghosh, K. K.; Ha, H. H.; Kang, N. Y.; Chandran, Y.; Chang, Y. T. *Chem. Commun.* **2011**, *47*, 7488.